Asian Journal of Chemistry; Vol. 36, No. 11 (2024), 2569-2574

ASIAN JOURNAL OF CHEMISTRY

https://doi.org/10.14233/ajchem.2024.32572

Preparation of Polycarbazole and Polyaniline Conducting Thin Films and Coating on Indium Tin Oxide by Spin Coating, Dip Coating and Drop Casting

A. ANNAM RENITA[1,*], SUNITHA SALLA[1], N.R. KRISHNAMOORTHY[1], P. KANAKARAJU[2], K. SANGEETHA[2], S. SELVAKUMAR[2], D. GOKUL[2] and ANKIREDDY GIRIDHAR[2]

[1]Department of Chemistry, Sathyabama Institute of Science and Technlogy, Chennai-600119, India
[2]SDSC-SHAR, Indian Space Research Organization, Sriharikota-524124, India

*Corresponding author: E-mail: reniriana@gmail.com

Received: 23 August 2024; *Accepted*: 12 October 2024; *Published online*: 30 October 2024; AJC-21791

Conducting polymers such as polyaniline (PANI), polycarbazole (PC) and polythiophene (PT) have gained attraction among researchers owing to their outstanding electrical and optical properties. In present study, polyaniline (PANI), polycarbazole (PC) and polythiophene (PT) were prepared by oxidative chemical polymerization followed by their characterization using techniques such as Fourier transform infrared spectroscopy (FTIR), X-ray diffractometry (XRD), scanning electron microscopy (SEM), electrochemical impedance spectroscopy (EIS) and Raman spectroscopy. The synthesized polymers were further coated with indium tin oxide (ITO) using three different methods *viz*. spin coating, dip coating and drop casting. The thickness of the films was measured using a Stylus Profilometer and found to be 400 nm for PC and 500 nm for PANI and PT. Therefore, it can be concluded that using suitable process parameters, thin films can be easily obtained from conducting polymers, thus opening new avenues in their application towards sensors, supercapacitors and optoelectronic devices.

Keywords: Polycarbazole, Polyaniline, Polythiophene, Indium tin oxide, Spin coating, Drop casting, Dip coating.

INTRODUCTION

Conducting polymers (CPs), namely, polyaniline (PANI), polycarbazole (PC) and polythiophene (PT), along with their derivatives, have significant electronic and optical properties, stretchability, low cost, resistance to corrosion, stability, photoluminescence and sensor applications [1-3]. CPs form a unique class of sensing nanomaterials with interesting properties that suit the development of smart nanosensors [4-6]. PANI has a large surface area and is also easily dissolved in solvents such as ketone, alcohol and other PANI-based organic solvents [7]. Besides, PANI has outstanding thermal stability and good optical and electrical properties [8-11]. Hence, they are used to manufacture semiconductors, organic light-emitting diodes (OLED) and organic solar cells [12,13].

Polycarbazole (PC) and their derivatives have been used for the last 50 years because of their excellent stability and greater redox potential compared to other CPs [14,15]. Moreover, they have good photoactive properties as they are hole transport materials with high mobility and exhibit stronger absorption in the UV spectral region [16,17]. The above characteristics enable them to be applied in transistors, light-emitting diodes, biosensors and photovoltaic devices [18,19]. Apart from PC and PANI, PT is another CP that is well known for its energy storing and sensor applications. Further, they are applied in solar cells, flexible circuits and photovoltaic cells [20,21]. Sometimes, PTs are engineered to enhance sensory applications with respect to the detection of various kinds of biomolecules. Thus, they can substitute PCR-based detection of biomolecules [22].

The substrates for coating polymers can be made of almost any materials, such as metals, plastics and ceramics. Aluminium, copper, zinc alloys and galvanized steel are frequently used for coatings [23]. Indium tin oxide (ITO)-coated glass is greatly used as a conductive substrate in solar cells, light emitting diodes (LEDs) and other electrochromic devices (ECD) [24,25]. For example, in one of the previous studies, a carbazole derivative, namely 9-methyl-9*H*-carbazole-3,6-diamine (m-Cz-diamine), was attached *via* covalent bonding onto the surface of an ITO

substrate usingdiazonium electro-reduction method. The resultant electrografted films showed excellent adhesion on the ITO surface. In comparison to the ITO substrate alone, they were more flexible and strong, and they remained intact when subjected to external forces [26]. Zhu [27] used PANI films on ITO substrate produced for electrochemical sensing of *p*-nitrophenol. Another study reported polythiophene (PT) based π-conjugated polymer production where PT units were substituted with cyano groups [21]. The power conversion efficacy of the solar cell produced using PT polymer was much higher than that of other polymers and also it has a greater short circuit current density of 0.11 mA cm^{-2}.

Further, the polymer possesses high charge carrier mobility, thus enabling us to utilize the polymer in different fields [28]. Besides, it was evident from the previous studies that PC, PANI and PT films coated on ITO substrates exhibit excellent physico-chemical and electrochemical properties. Consequently, they are significantly more appropriate for sensor fabrication. Few studies have been conducted on the synthesis and characterization of PC, PANI and PT films on ITO glass substrates that can be used to fabricate sensors. Furthermore, different synthetic methods such as drop casting, dip coating and further post-treatment methods enhanced the electrical conductivity of the synthesized films. Therefore, this research aims to produce thin films of PC, PANI and PT, which can be further coated on ITO glass substrate using spin coating, dip coating and drop casting. The synthesized film coated on ITO glass substrate was characterized using techniques such as Fourier transform infrared spectroscopy (FTIR), X-ray diffractometry (XRD), scanning electron microscopy (SEM), energy-dispersive X-ray (EDX) and Raman spectroscopy. Further in this work, the thickness of the film is measured using a Stylus profilometer.

EXPERIMENTAL

Carbazole, aniline, chloroform, methanol, sulphuric acid, acetonitrile and *N*,*N*-dimethylformamide (DMF) and dimethyl sulfoxide (DMSO) were purchased from Merck Pvt. Ltd and used without purification. Polymers were characterized using SEM (FlexSEM 1000, Hitachi, Japan) and FTIR (PE IR SPECTRUM ASCII PEDS 1.60 spectrometer).

Synthesis of polycarbazole (PC): Carbazole (0.5 g) was added to 50 mL of acetonitrile in a beaker and magnetic stirred for 15 min. In another beaker, 0.8 g of ammonium persulphate and 8 mL of acetonitrile were mixed while stirring for 15 min. The contents in both the beakers were mixed and stirred the solution for 30 min. The resultant black solution was mixed with methanol and then filtered using a Whatmann filter paper. The precipitate was dried and kept for further analysis.

Synthesis of polyaniline (PANI): A 15 mL of conc. H_2SO_4 was added dropwise to 20 mL of aniline followed by the addition of 25 mL of potassium dichromate solution and then the mixture was stirred for 3.5 h. The resultant mixture was filtered and the precipitate was dried.

Synthesis of polythiophene (PT): A 40 mL chloroform and 0.4 g of sodium dodecyl sulfate (SDS) was mixed properly. In another beaker, 2.8 g of $FeCl_3$ and 90 mL of chloroform were mixed. Then both contents were mixed and stirred continuously for 30 min followed by the slow addition of 30 mL of thiophene and stirred for 6 h. The resultant solution was filtered and the solid product was filtered again using doping method.

Coating methods

Drop casting: The electrochemical conducting films were synthesized by dissolving the polymers into DMSO and DMF. The polymers were taken in different beakers,each adding a different DMSO concentration and stirred well. Then, the solution was transferred into a closed container and kept in an ultrasonic bath for 1.0-1.5 h. Then, they were evaluated by spin coating and drop casting techniques to coat on ITO substrate. The solvent was evaporated for 10-12 h in a dry vacuum. The coat solution was dropped on the substrate to be coated and heat was applied to the substrate to be coated in this procedure. The heat caused the solvent to evaporate spontaneously and the substrate was allowed to cool after the coat had been dropped and settled. A film was formed when the polymer coating was completely cooled. The thickness of the film was determined by the volume of dispersion used and the particle concentration, both of which are easily adjustable. Other factors that influenced the film structure include the ability of solvent to wet the substrate, evaporation rate and drying capillary forces. In terms of usage, the drop casting technique was very simple and material waste was minimal.

Dip coating: In dip coating technique, the materials were dipped in the solution and left for drying, which was a simple procedure. Other factors that affect the film substrate include the ability of solvent to wet the substrate, evaporation rate and drying capillary forces. Water is considered to be a poor solvent for drop casting due of its low vapour pressure and high surface tension. The solvents DMSO and DMF were used to prepare the polymer mixture.

Spin coating: In spin coating technique, the substrate to be coated was placed in the holder unit of the spin coater. The required amount of conducting polymer was dropped over the substrate surface and the software integrated with the spin coater adjusted the rpm. The time and rpm were fixed and the program was run to get the desired thin films.

Thickness of film: In order to measure the thickness (or height) of a film's surface, stylus profilometers physically move a probe along the surface. This was done mechanically with a feedback loop that monitored the force from the sample pushing up against the probe as it scanned along the surface. Silane was used as binder for better adherence of PC, PANI and PT films to the ITO substrate. The device involved physical movements in X, Y and Z while maintaining contact with the surface; hence, it is considered slower than non-contact techniques. The stylus tip size and shape can influence the measurements and limit the lateral resolution.

RESULTS AND DISCUSSION

Morphological studies: Fig. 1a-b shows the SEM images of PANI and PC polymers. The surface profile and morphologies can be observed in scanning electron micrographs (SEM) taken during polymer synthesis. PANI was prepared using modified Hummers's method [29] and the granular morphology of PANI

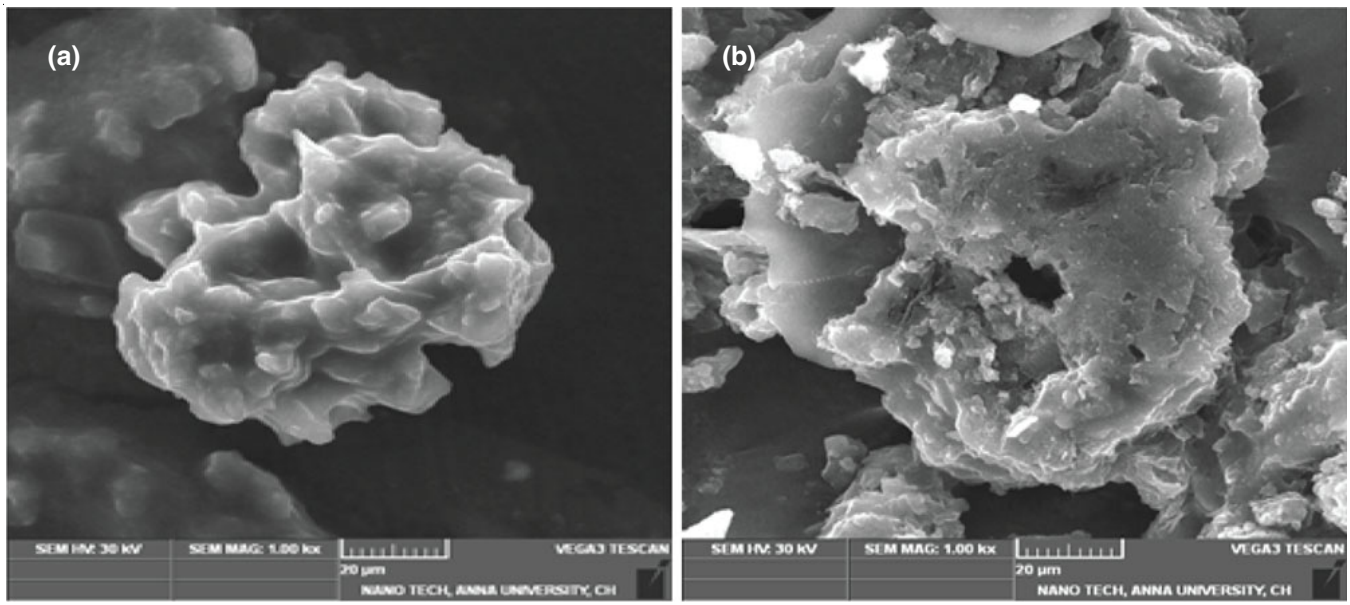

Fig. 1. SEM image of (a) PANI and (b) PC

powders is the most common in PANI prepared by precipitation polymerization when using strong oxidants and high aniline concentrations under strongly-acidic conditions at pH < 2.5. PANI is a conducting polymer and is sensitive to temperature during the SEM analysis. When the sample interacts with electrons, it will generate a small amount of heat, leading to cracks in the samples [30]. The SEM image clearly shows the particles, which are both well-defined and extremely scattered, with some aggregation. The aggregation of these particles is due to the effect of heating. All the particles are spherical in shape and slightly agglomerated. On the other hand, the SEM image of PC (Fig. 1b) indicates that the polymer has an irregular shape with sizes of about several micrometres and shows good conductivity in time delay and integration (TDI) detection.

EDX was done to study the prepared polymers' chemical composition and the weight percentages are given in Table-1, which shows that PANI has more elements when compared to that of PC. While PANI has more weight and atomic % of carbon (39.29% and 49.16%, respectively), PC has more weight and atomic % of oxygen (28.53% and 28.32%, respectively) and sulphur (23.14% and 11.46%, respectively). A slight difference was found with respect to the composition of nitrogen. Further,

TABLE-1
EDX ANALYSIS OF PANI AND PC

Element	Weight (%)		Atomic (%)	
	PANI	PC	PANI	PC
C	39.29	28.86	49.16	38.15
N	18.81	19.47	20.18	22.08
O	23.82	28.53	22.37	28.32
S	17.11	23.14	8.02	11.46
Cr	0.43	–	0.13	–
Fe	0.55	–	0.15	–

PANI also consist of trace amounts of Cr (0.43%) and Fe (0.55%), however, they are absent in PC. The elemental composition shows that both PANI and PC-based polymers can be applied in the field of sensors because of their outstanding conductive properties.

Raman spectra: Fig. 2a-c show the Raman spectra of PANI, PC and PT, respectively. In Fig. 2a, the characteristic bands were observd at 1170 (C-H *bend.*), 1206 (C-N *str.*), 1502 (C=N *str.*); 1560 (N-H *bend.*) and 1598 cm^{-1} (C=C *str.*). The conductivity of PANI is due to the band at 890 cm^{-1}, which is assigned to the deformation of C-N of secondary amine next to aromatic ring in the polaronic form C-N^{+}-C and to the band

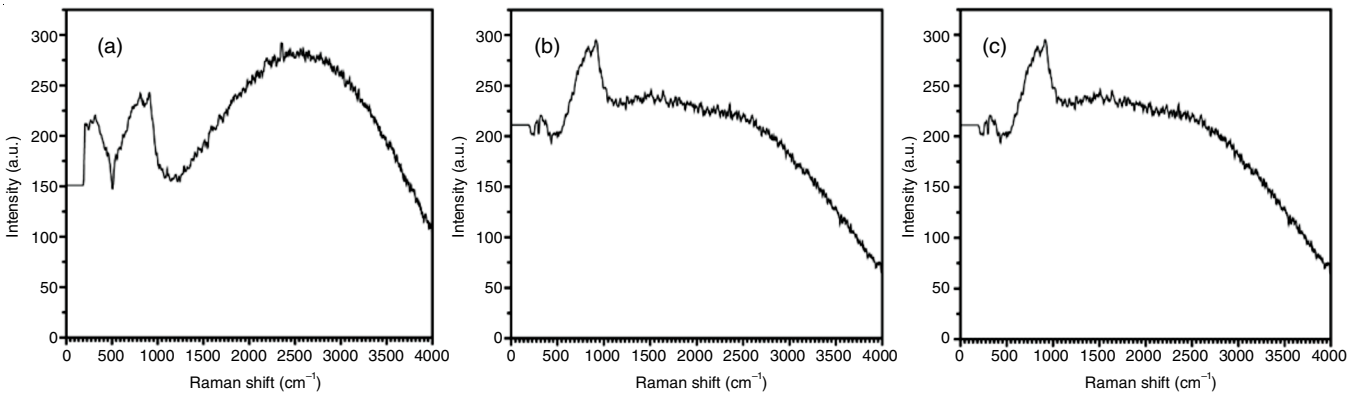

Fig. 2. Raman spectra of (a) PANI, (b) PC and (c) PT

at 1343 cm^{-1} [31]. This is attributed to the vibration of a delocalized polaron structure. In Fig. 2b, the absorption band at 1016 cm^{-1} is for C-O stretching and absorption band at 1378 cm^{-1} is attributed to aromatic C-H bending. Further, the band at 1520 cm^{-1} is due to C=C stretching and a band at 1605 cm^{-1} is due to C=O stretching [32]. In Fig. 2c, the most important peak of PT is observed at 1422 cm^{-1} which can be attributed to the Cα=Cβ backbone ring stretching of the neutral PT [33]. The peak at 1390 cm^{-1} is because of the bipolaron absorption band and Cβ-H bending appears at 1066 cm^{-1}. The band located at about 728 to 702 cm^{-1} is assigned to the C-S-C ring deformation associated with dication (bipolaron) and radical cation (polaron), respectively. The peaks at 1221 cm^{-1} and 1325 cm^{-1} are assigned to Cα–Cα′ stretching and Cβ–Cβ′ ring stretching formations, respectively.

XRD spectra: Generally PANI films are semi-crystalline in nature and have a 2θ-phase system. The phase in which the polymer chains are parallel and ordered in a closely packed array is considered to be the crystallite region. On the other hand, the phase where the chains are not ordered and do not have parallel alignment is the amorphous region [34]. Fig. 3a shows the XRD pattern of PANI and the crystalline phase can be identified in XRD spectra at 2θ = 18º, 20º, 21º and 24º, which proves it to be a more ordered structure. The XRD pattern of PC is presented in Fig. 3b and consists of three prominent peaks at 18º, 23º, 26º and three small peaks at 50º, 57º, 70º. The XRD pattern exhibits sharp diffraction peaks at 18º, 23º and 26º, ascribed to the periodicity parallel to the polymer chain. In contrast, the weak peaks at high angles may be caused by periodicity perpendicular to the polymer chain.

FTIR spectra: The results of the FT-IR measurement of PANI are exhibited in Fig. 4a. The peaks at 1562 and 1479 cm^{-1} correspond to the stretching modes of ν(C=C) strain on the quinonoid ring and ν(C=C) on the benzenoid ring. The peak at 1479 cm^{-1} is observed lower than at 1560 cm^{-1}, hence, it can be understood that the synthesized PANI has a lesser number of benzenoid rings than the quinoid rings. Additionally, the peak on 1302 cm^{-1} and 1246 cm^{-1} area was assigned to ν(C-N) stretching of secondary aromatic amine and ν(C-$N^{+\bullet}$) stretching on the polar one lattice, respectively.

The FTIR spectrum of PC (Fig. 4b) shows a strong and broad band at 3401 cm^{-1}, which is assigned to the O-H group. All the peaks are broader after electrochemical oxidation, as shown for the N-H group, which was shifted to 3547 cm^{-1}. The IR spectrum of PC at 2243 cm^{-1} is attributed to the nitrile group, whereas the peaks at 2956 cm^{-1} and 2869 cm^{-1} is attributed to the C-H stretching vibration mode. The band at 1600-1400 cm^{-1} spectral range is assigned to an aromatic ring and the band at 1325 cm^{-1} is attributed to the CH_2 group. The band at 1191 cm^{-1} and 1325 cm^{-1} is attributed to the C-N and C-C

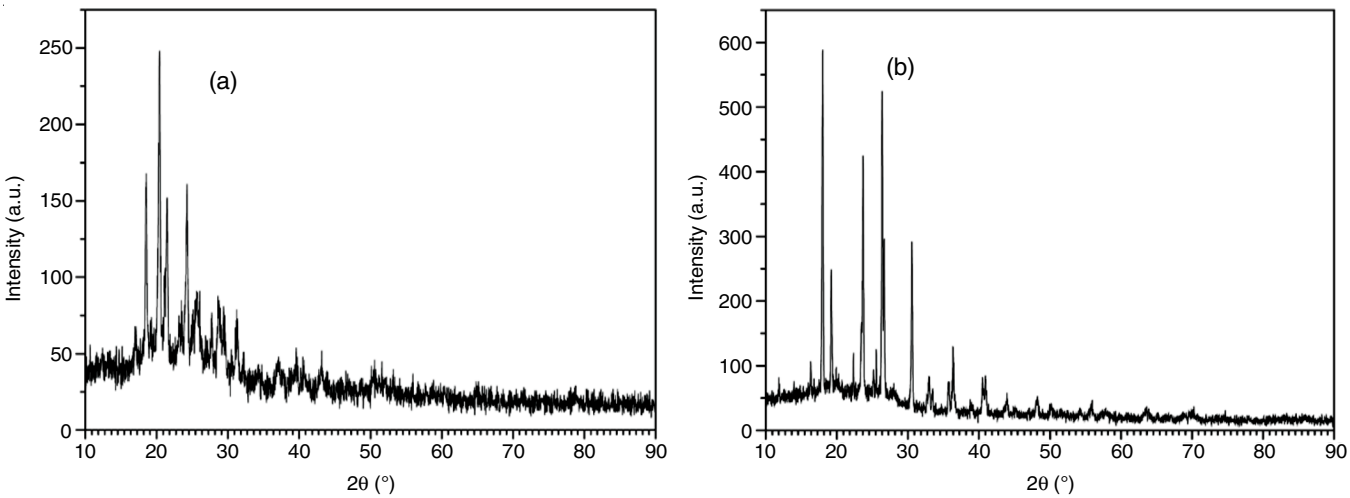

Fig. 3. XRD image of (a) PANI and (b) PC

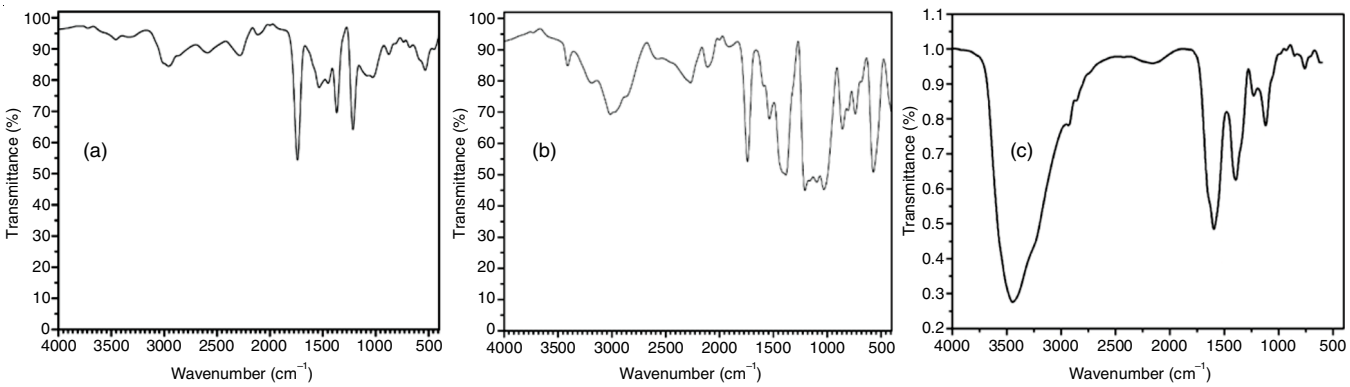

Fig. 4. FTIR spectra of (a) PANI, (b) PC and (c) PT

groups, respectively. The band at 1620 cm^{-1} may be attributed to the C=O group and the band at 1215 cm^{-1} is attributed to the C-O group.

The chemical structures of PT thin film sample were determined by the FTIR spectroscopy study, which is represented in Fig. 4c. The absorption band in the region 2920.03 cm^{-1} is due to the aromatic C=C-H stretching frequency. The major peaks observed at 1705.95 cm^{-1} and 1538.25 cm^{-1} are assigned for C=C asymmetric and symmetric stretching vibration of the thiophene ring. The bands at 1361.91 cm^{-1} to 1077.77 cm^{-1} are due to the deformation of C-H bending and CH in-plane of vibrations. The peaks at 793.54 cm^{-1}, 644.98 cm^{-1}, 544.76 cm^{-1} and 481.13 cm^{-1} are assigned for the C-S bending vibration and C-S-C ring deformation stretching of PT, which confirms the successful polymerization of thiophene monomer and the formation of polythiophene.

Coating of synthesized polymers: The thickness of PANI, PC and PT films along with the methodology adopted for coating are presented in Table-2. It can be observed that the thickness of PANI and PT remains the same (500 nm), whereas the thickness of PC was slightly lower (400 nm). The electrical properties of the synthesized films largely depend on the thickness of the films. Kim *et al.* [35] stated that there was an inverse relationship existed between film resistance and thickness. One of the previously conducted studies observed that when the thickness of PEDOT:PSS/Tween 80 films increased, the resistance values of the sheet started to decrease [36].

TABLE-2
THICKNESS OF THE POLYMER FILMS AND THEIR METHODOLOGY OF PRODUCTION

Film	Method used	Thickness (nm)
PANI	Spin coating	500
PC	Spin coating	400
PT	Dip coating	500

Further, in another study, with respect to polyimide films, when the values of thin film thickness ranged from 100 to 200 nm, the values of thermal conductivity were found to be 0.3 $W\ m^{-1}\ K^{-1}$. The films' electrical properties were evaluated using a time-domain thermoreflectance system. It was observed that the film with a thickness of 40 nm has more thermal conductivity of ~0.60 $W\ m^{-1}\ K^{-1}$. This is approximately three times more than the thermal conductivity of a commercially available pristine PEDOT:PSS film of the same thickness [37]. Hence, it was evident from the previous reports that the polymer films' thermal resistance (inverse of conductivity) decreased when the thickness increased.

Conclusion

Conducting polymers (CPs) consisted of polyaniline (PANI), polycarbazole (PC) and polythiophene (PT) were prepared prepared using standard procedures. The polymers were characterized by SEM, EDX, Raman spectra, XRD and FTIR. All polymer samples were characterized in both powder and thin film forms, and their presence was confirmed. Dip, drop, and spin coating were the three methods used for coating the polymers on the ITO films. The PANI and PT films possess a thickness of 500 nm and PC film has a thickness of 400 nm as evaluated from Stylus profilometer. It was concluded that when the film thickness increased, the film's resistance decreased. Thus, the thin films coated on ITO glass substrate find their applications in producing energy storage devices, batteries, electronic systems, sensors, anticorrosion coating instruments and other organic photovoltaic cells.

CONFLICT OF INTEREST

The authors declare that there is no conflict of interests regarding the publication of this article.

REFERENCES

1. T.V. Nguyen, Q.V. Le, S. Peng, Z. Dai, S.H. Ahn and S.Y. Kim, *Adv. Mater. Technol.*, **8**, 2300474 (2023); https://doi.org/10.1002/admt.202300474
2. M.G. Tadesse, A.S. Ahmmed and J.F. Lübben, *J. Compos. Sci.*, **8**, 53 (2024); https://doi.org/10.3390/jcs8020053
3. S. Tajik, H. Beitollahi, F.G. Nejad, I.S. Shoaie, M.A. Khalilzadeh, M.S. Asl, Q. Van Le, K. Zhang, H.W. Jang and M. Shokouhimehr, *RSC Adv.*, **10**, 37834 (2020); https://doi.org/10.1039/D0RA06160C
4. C.S. Park, C. Lee and O.S. Kwon, *Polymers*, **8**, 249 (2016); https://doi.org/10.3390/polym8070249
5. E.A. Ryan, Z.D. Seibers, J.R. Reynolds and M.L. Shofner, *J. Appl. Polym. Sci.*, **55**, 225 (2024); https://doi.org/10.1002/app.55225
6. A. Rehman and X. Zeng, *Curr. Opin. Electrochem.*, **23**, 47 (2020); https://doi.org/10.1016/j.coelec.2020.03.010
7. E. Eskandari, M. Kosari, M.H. Davood Abadi Farahani, N.D. Khiavi, M. Saeedikhani, R. Katal and M. Zarinejad, *Sep. Purif. Technol.*, **231**, 115901 (2020); https://doi.org/10.1016/j.seppur.2019.115901
8. N. Chandrakanthi and M.A. Careem, *Polym. Bull.*, **44**, 101 (2000); https://doi.org/10.1007/s002890050579
9. S. Shahabuddin, R. Gaur, N. Mukherjee, P. Chandra and R. Khanam, *Mater. Today Proc.*, **62**, 6950 (2022); https://doi.org/10.1016/j.matpr.2021.12.335
10. F. Kazemi, S.M. Naghib, Y. Zare and K.Y. Rhee, *Polym. Rev.*, **61**, 553 (2021); https://doi.org/10.1080/15583724.2020.1858871
11. S.S. Shah, S. Oladepo, M.A. Ehsan, W. Iali, A. Alenaizan, M.N. Siddiqui, M. Oyama, A.-R. Al-Betar and M.A. Aziz, *Chem. Rec.*, **24**, e202300105 (2024); https://doi.org/10.1002/tcr.202300105
12. A. Saraswat and S. Kumar, *Eur. Polym. J.*, **200**, 112501 (2023); https://doi.org/10.1016/j.eurpolymj.2023.112501
13. M. Beygisangchin, S.A. Rashid, S. Shafie, A.R. Sadrolhosseini and H.N. Lim, *Polymers*, 13, 2003 (2021); https://doi.org/10.3390/polym13122003
14. X. Liu, W. Zheng, R. Kumar, M. Kumar and J. Zhang, *Coord. Chem. Rev.*, **462**, 214517 (2022); https://doi.org/10.1016/j.ccr.2022.214517
15. A. Et Taouil, S. Lakard, F. Dumur, E. Contal and B. Lakard, *Synth. Met.*, **300**, 117491 (2023); https://doi.org/10.1016/j.synthmet.2023.117491
16. J. Bhadra, A. Alkareem and N. Al-Thani, *J. Polym. Res.*, **27**, 122 (2020); https://doi.org/10.1007/s10965-020-02052-1
17. E. Contal, S. Lakard, F. Dumur and B. Lakard, *Prog. Org. Coat.*, **162**, 106563 (2022); https://doi.org/10.1016/j.porgcoat.2021.106563
18. F. Coban, R. Ayranci and M. Ak, *Synth. Met.*, **296**, 117356 (2023); https://doi.org/10.1016/j.synthmet.2023.117356

19. F. Bekkar, F. Bettahar, I. Moreno, R. Meghabar, M. Hamadouche, E. Hernáez, J.L. Vilas-Vilela and L. Ruiz-Rubio, *Polymers*, **12**, 2227 (2020); https://doi.org/10.3390/polym12102227
20. S.S. Shindalkar, M. Reddy, R. Singh, M.A.M. Nainar and B. Kandasubramanian, *Synth. Met.*, **299**, 117467 (2023); https://doi.org/10.1016/j.synthmet.2023.117467
21. W. Zhang, C. Zhang, J. Liu, X. Wang and S. Zhu, *Sol. Energy Mater. Sol. Cells*, **251**, 112146 (2023); https://doi.org/10.1016/j.solmat.2022.112146
22. B. Gangopadhyay, A. Roy, D. Paul, S. Panda, B. Das, S. Karmakar, K. Dutta, S. Chattopadhyay and D. Chattopadhyay, *ACS Appl. Bio Mater.*, **7**, 485 (2024); https://doi.org/10.1021/acsabm.3c01126
23. Z. Yu, J. Hu and H. Meng, *Front. Mater.*, **7**, 74 (2020); https://doi.org/10.3389/fmats.2020.00074
24. R. Hu, X. Su, H. Liu, Y. Liu, M.M. Huo and W. Zhang, *J. Mater. Sci.*, **55**, 11403 (2020); https://doi.org/10.1007/s10853-020-04825-x
25. K. Krukiewicz, D. Czerwiñska-G³ówka, R.M. Turczyn, A. Blacha-Grzechnik, C. Vallejo-Giraldo, K. Erfurt, A. Chrobok, J. Faure-Vincent, S. Pouget, D. Djurado and M.J.P. Biggs, *ACS Appl. Mater. Interfaces*, **15**, 45701 (2023); https://doi.org/10.1021/acsami.3c10861
26. A. Kumar, E. Contal, S. Lakard, F. Dumur, R. Meunier-Prest, L. Viau, M. Bouvet and B. Lakard, *Surf. Interfaces*, **35**, 102447 (2022); https://doi.org/10.1016/j.surfin.2022.102447
27. G. Zhu, Q. Tang, M. Huang, J. Yang, R. Xu and J. Liu, *Sens. Actuators B Chem.*, **320**, 128593 (2020); https://doi.org/10.1016/j.snb.2020.128593
28. I. Kang, H.-J. Yun, D.S. Chung, S.-K. Kwon and Y.-H. Kim, *J. Am. Chem. Soc.*, **135**, 14896 (2013); https://doi.org/10.1021/ja405112s
29. Y. Wang, Y. Wang, Y. Tian, L. Ma, C. Wang and X. Gao, *ECS J. Solid State Sci. Technol.*, **8**, M103 (2019); https://doi.org/10.1149/2.0231910jss
30. J. Song, Y. Wei, M. Xu, J. Gao, L. Luo, H. Wu, X. Li, Y. Li and X. Wang, *ACS Appl. Polym. Mater.*, **4**, 766 (2022); https://doi.org/10.1021/acsapm.1c01224
31. M.A.C. Mazzeu, L.K. Faria, A.D.M. Cardoso, A.M. Gama, M.R. Baldan and E.S. Gonçalves, *J. Aerosp. Technol. Manag.*, **9**, 39 (2017); https://doi.org/10.5028/jatm.v9i1.726
32. M. Shakir, Noor-e-Iram, M.S. Khan, S.I. Al-Resayes, A.A. Khan and U. Baig, *Ind. Eng. Chem. Res.*, **53**, 8035 (2014); https://doi.org/10.1021/ie404314q
33. S. Sakthivel and A. Boopathi, *Int. J. Sci. Res.*, **141**, 97 (2014).
34. F. Saouti, S. Belaaouad, A. Cherqaoui and Y. Naimi, *Biointerface Res. Appl. Chem.*, **12**, 5523 (2021); https://doi.org/10.33263/BRIAC124.55235533
35. S. Kim, A. Konar, W.S. Hwang, J.H. Lee, J. Lee, J. Yang, C. Jung, H. Kim, J.-B. Yoo, J.-Y. Choi, Y.W. Jin, S.Y. Lee, D. Jena, W. Choi and K. Kim, *Nat. Commun.*, **3**, 1011 (2012); https://doi.org/10.1038/ncomms2018
36. J.L. Carter, C.A. Kelly, J.E. Marshall, V. Hammond, V. Goodship and M.J. Jenkins, *Polymers*, **14**, 5072 (2022); https://doi.org/10.3390/polym14235072
37. J.L. Carter, C.A. Kelly, J.E. Marshall and M.J. Jenkins, *Polym. J.*, **56**, 107 (2023); https://doi.org/10.1038/s41428-023-00854-w